IOPscience iopscience.iop.org

Home Search Collections Journals About Contact us My IOPscience

Depolarization artifacts in dual rotating-compensator Mueller matrix ellipsometry

This content has been downloaded from IOPscience. Please scroll down to see the full text.

2016 J. Opt. 18 055701

(http://iopscience.iop.org/2040-8986/18/5/055701)

View the table of contents for this issue, or go to the journal homepage for more

Download details:

IP Address: 211.69.194.151
This content was downloaded on 16/03/2016 at 11:45

Please note that terms and conditions apply.

IOP Publishing | Journal of Optics
J. Opt. 18 (2016) 055701 (7pp) | doi:10.1088/2040-8978/18/5/055701

Depolarization artifacts in dual rotating-compensator Mueller matrix ellipsometry

Weiqi Li[1], **Chuanwei Zhang**[1,2], **Hao Jiang**[1,3], **Xiuguo Chen**[1] **and Shiyuan Liu**[1,2,3]

[1] State Key Laboratory of Digital Manufacturing Equipment and Technology, Huazhong University of Science and Technology, Wuhan 430074, People's Republic of China
[2] Wuhan Eoptics Technology Co. Ltd, Wuhan 430075, People's Republic of China

E-mail: hjiang@hust.edu.cn and shyliu@hust.edu.cn

Received 15 October 2015, revised 19 December 2015
Accepted for publication 15 January 2016
Published 14 March 2016

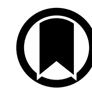

Abstract
Noticeable depolarization effects are observed in the measurement of the air using an in-house developed dual rotating-compensator Mueller matrix ellipsometer. We demonstrate that these depolarization effects are essentially artifacts and mainly induced when the compensator with wavelength-dependent optical properties is integrated with the finite bandwidth detector. We define a general formula to represent the actual Mueller matrix of the compensator by taking into account the depolarization artifacts. After incorporating this formula into the system model, a correction method is further proposed, and consequently, improved accuracy can be achieved in the Mueller matrix measurement.

Keywords: depolarization, dual rotating-compensator, Mueller matrix ellipsometry, finite bandwidth, correction, measurement accuracy

(Some figures may appear in colour only in the online journal)

1. Introduction

Recently, Mueller matrix ellipsometry (MME) has been applied as a powerful tool for the characterization of optically anisotropic materials [1–3], diffractive nanostructures [4–6], and depolarization effects [7, 8]. Among the various types of MME, dual rotating-compensator (DRC) based configuration is a popular one due to its broad band, low cost, and relative simplicity of operation and calibration. One of the key components in the DRC-MME system is the rotating compensator, which is apt to induce apparent systematic errors. Existing methods to deal with such systematic errors are all focused on the azimuthal angle error and retardance error of the compensator [9–12]. The effects when the compensators are integrated with other optical components in the MME system are rarely explored and usually ignored, which may lead to noticeable accuracy loss in the Mueller matrix measurement.

In this work, we investigate the depolarization effects observed in the measured Mueller matrix of the air obtained by an in-house developed DRC-MME system in a straight-through mode. Since the air has no depolarization effect, the observed depolarization effects are essentially artifacts induced by the MME system. We demonstrate that these depolarization effects are mainly induced when the compensator, especially the composite-waveplates type compensator with wavelength-dependent optical properties, is integrated with the finite bandwidth monochromator or detector. By taking into account the depolarization artifacts, we define a general formula to represent the actual Mueller matrix of the compensator. By incorporating this formula into the system model, we further propose a correction method to eliminate the depolarization artifacts.

2. Observation of depolarization artifacts in DRC-MME

As schematically shown in figure 1, the basic system layout of the DRC-MME in order of light propagation is $PC_{r1}(\omega_1)SC_{r2}(\omega_2)A$, where P and A stand for the polarizer and analyzer, C_{r1} and C_{r2} refer to the 1st and 2nd rotating compensators, and S stands for the sample. The fast axis angle C_1 and

[3] Authors to whom any correspondence should be addressed.

 © 2016 IOP Publishing Ltd Printed in the UK

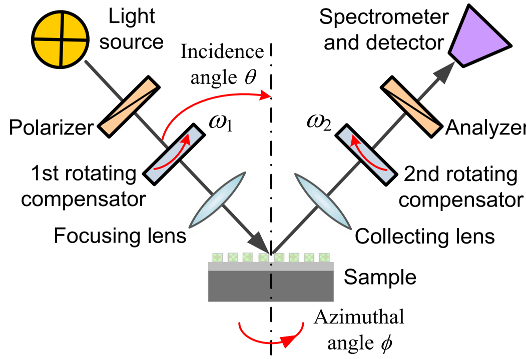

Figure 1. Principle and prototype of the dual rotating-compensator Mueller matrix ellipsometer.

C_2 of the 1st and 2nd compensators rotate synchronously at $\omega_1 = 5\omega$ and $\omega_2 = 3\omega$, where ω is the fundamental mechanical frequency. The emerging Stokes vector $\mathbf{S}_{\text{out}}$ of the exiting light beam can be expressed as the following Mueller matrix product [13]:

$$\begin{aligned}\mathbf{S}_{\text{out}} = &[\mathbf{M}_A\mathbf{R}(A)][\mathbf{R}(-C_2)\mathbf{M}_{C_2}(\delta_2)\mathbf{R}(C_2)]\\ &\times \mathbf{M}_S \times [\mathbf{R}(-C_1)\mathbf{M}_{C_1}(\delta_1)\mathbf{R}(C_1)]\\ &\times [\mathbf{R}(-P)\mathbf{M}_P\mathbf{R}(P)]\mathbf{S}_{\text{in}},\end{aligned} \tag{1}$$

where $\mathbf{M}_i$ ($i = P, A, C_1, C_2$) is the Mueller matrix associated with each optical element. $\mathbf{R}(\alpha)$ is the Mueller rotation transformation matrix for rotation by the angle α ($\alpha = P, A, C_1, C_2$) that describes the corresponding orientation angle of each optical element. δ_1 and δ_2 are the wavelength-dependent phase retardances of the 1st and 2nd rotating compensators. By multiplying the matrices in equation (1), we can obtain the following expression for the irradiance at the detector (proportional to the first element of $\mathbf{S}_{\text{out}}$) [13]:

$$\begin{aligned}I(t) = I_0\Bigg\{1 + \sum_{n=1}^{16}[\alpha_{2n}\cos(2n\omega t - \phi_{2n})\\ + \beta_{2n}\sin(2n\omega t - \phi_{2n})]\Bigg\},\end{aligned} \tag{2}$$

where I_0, α_{2n} and β_{2n} are the dc and d.c-nomalized ac harmonic coefficients, respectively. The sample Mueller matrix elements m_{ij} ($i, j = 1, 2, 3, 4$) are linear combinations of α_{2n} and β_{2n}. By performing Fourier analysis [14], the Mueller matrix elements of the sample can be extracted from these harmonic coefficients. Based on the above measurement principle, we developed a DRC-MME prototype [15]. The spectral range is from 200 to 1000 nm with a bandwidth of 3.5 nm. The beam diameter can be changed from the nominal value of ~3 mm to a value of ~200 μm equipped with the focusing lens. The small beam size is particularly used when the area for detection is smaller than the nominal beam size, and the finite numerical aperture of the focusing lens will lead to a sample-dependent depolarization effect, which is usually considered in the theoretical ellipsometric data calculation of samples [8, 15]. In order to investigate the effects purely induced by the instrument, the nominal beam size is used in the present experiments. Achromatic compensators made of composite waveplates are used in our system to achieve an approximate retardance angle of the optimal 127° over the entire spectral range [16]. The two arms of the instrument can be rotated to change the incidence angle in experiments. When rotating the arms at 90° incidence angle, i.e., in the straight-through measurement mode, the full 4 × 4 Mueller matrix of the air can be acquired, which should be a 4 × 4 identity matrix for an ideal system. If systematic errors exist, the measured Mueller matrix of the air will deviate from the identity matrix. This provides a simple and effective way to assess the measurement accuracy of MME systems. Figure 2 shows the measured Mueller matrix spectra of the air, from which noticeable deviation from the identity matrix can be observed. It reveals that systematic errors exist and degrade the Mueller matrix measurement accuracy. In particular, the error is up to 2% within the spectral range, and the standard deviation is about 0.7%. We will demonstrate that the systematic errors are caused by the depolarization effects when the compensators are integrated with the finite bandwidth detector.

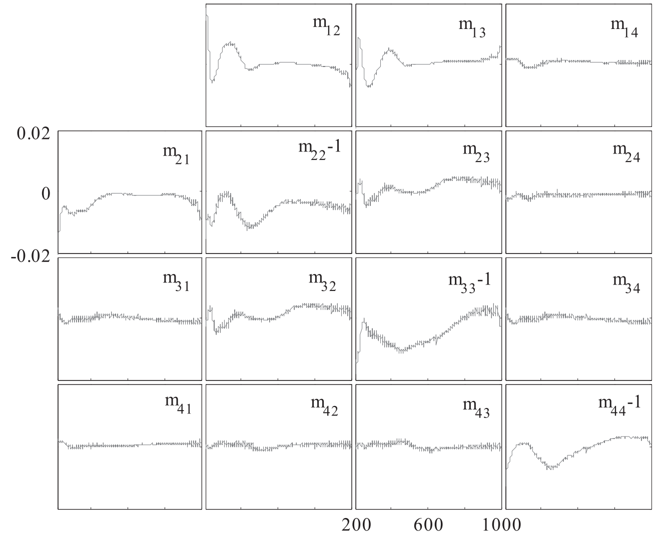

Figure 2. Mueller matrix spectra of the air measured by the in-house developed DRC-MME. The Mueller matrix elements are normalized to m_{11}, which is not shown. The horizontal axes, varying from 200 to 1000 nm, denote the wavelengths, and the vertical axes denote the values of the associated Mueller matrix elements. The diagonal elements m_{22}, m_{33} and m_{44} are minus 1 for the convenience of unified coordinate axis.

The depolarization effect is referred to as a physical phenomenon when totally polarized incident light is transformed into partially polarized light after interacting with an optical media, and the associated Mueller matrix becomes a

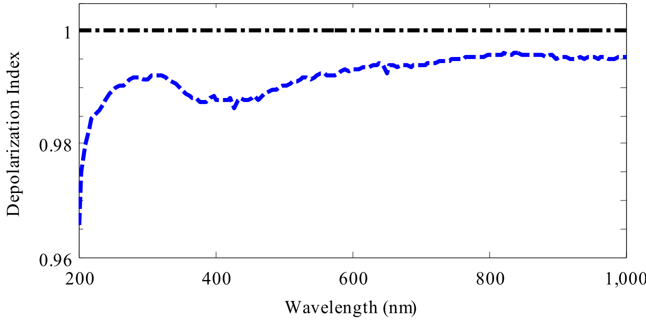

Figure 3. Depolarization index spectrum of the ellipsometer-measured Mueller matrix data.

depolarizing one. The depolarization effect can be described by the depolarization index DI that is defined by [17]:

$$DI = \left[\frac{\mathrm{Tr}(\mathbf{M}\mathbf{M}^{\mathrm{T}}) - m_{11}^2}{3m_{11}^2}\right]^{1/2}, \quad 0 \leqslant DI \leqslant 1 \tag{3}$$

where m_{11} is the (1, 1)th element of the Mueller matrix $\mathbf{M}$, $\mathbf{M}^{\mathrm{T}}$ is the transposed matrix of $\mathbf{M}$, and $\mathrm{Tr}(\cdot)$ represents the trace. $DI = 0$ and $DI = 1$ correspond to a totally depolarizing and non-depolarizing Mueller matrix, respectively. The depolarization index spectrum that corresponds to the measured Mueller matrix data shown in figure 2 is presented in figure 3. It is noted that the depolarization indices are close to 1 over the visible to near-infrared spectrum, but show obvious dips in the visible to ultraviolet range.

As the air itself does not induce depolarization effects, the observed depolarization effects are consequently caused by the MME system. Many factors may induce depolarization effects and can be classified overall into two categories, namely, the extrinsic and intrinsic factors [8]. The intrinsic factors include those that are closely related with the measured sample such as thickness nonuniformity, large surface or edge roughness, and thick transparent substrates. The extrinsic factors, such as the finite bandwidth of the monochromator or detector, and the finite numerical aperture of the focusing lens in the measurement system, induce depolarization effects in the measurement process. Assuming all the optical elements used in our MME system are perfectly manufactured, the elements themselves do not induce depolarization effects individually. However, since the composite waveplates are used as the rotating compensators whose optical properties such as the retardance, the fast-axis azimuthal angle, and the rotary angle are wavelength-dependent, the MME system induces depolarization effects in case the spectrograph bandwidth of the system is finite.

3. Modeling of depolarization artifacts in DRC-MME

The Mueller matrix corresponding to an ideal compensator is expressed by [18]:

$$\mathbf{M}(\delta_\lambda, \theta_\lambda) = \mathbf{R}(-\theta_\lambda)\mathbf{M}(\delta_\lambda)\mathbf{R}(\theta_\lambda), \tag{4}$$

where δ_λ and θ_λ denote the retardance and the fast-axis azimuthal angle of the compensator at wavelength λ respectively. The matrix $\mathbf{R}(\theta_\lambda)$ is the Mueller rotation transformation matrix expressed as:

$$\mathbf{R}(\theta_\lambda) = \begin{bmatrix} 1 & 0 & 0 & 0 \\ 0 & \cos 2\theta_\lambda & \sin 2\theta_\lambda & 0 \\ 0 & -\sin 2\theta_\lambda & \cos 2\theta_\lambda & 0 \\ 0 & 0 & 0 & 1 \end{bmatrix}, \tag{5}$$

and the Mueller matrix of the compensator in case the fast-axis is parallel to the x axis is given by

$$\mathbf{M}(\delta_\lambda) = \begin{bmatrix} 1 & 0 & 0 & 0 \\ 0 & 1 & 0 & 0 \\ 0 & 0 & \cos\delta_\lambda & \sin\delta_\lambda \\ 0 & 0 & -\sin\delta_\lambda & \cos\delta_\lambda \end{bmatrix}. \tag{6}$$

For the composite-waveplates type compensator used in our DRC-MME system, it can be optically equivalent to a cascaded system containing a pure waveplate and a rotator [19, 20]. Therefore, the Mueller matrix of the composite waveplates can be written as

$$\mathbf{M}(\delta_\lambda, \theta_\lambda, \rho_\lambda) = \mathbf{R}(\rho_\lambda)\mathbf{R}(-\theta_\lambda)\mathbf{M}(\delta_\lambda)\mathbf{R}(\theta_\lambda), \tag{7}$$

where ρ_λ is the rotary angle. When considering the finite bandwidth, the Mueller matrix of the composite waveplates becomes an integral expressed as

$$\overline{\mathbf{M}}(\lambda) = \int w(\lambda)\mathbf{R}(\rho_\lambda)\mathbf{R}(-\theta_\lambda)\mathbf{M}(\delta_\lambda)\mathbf{R}(\theta_\lambda)\mathrm{d}\lambda, \tag{8}$$

where $w(\lambda)$ is the spectral bandwidth function normalized as $\int w(\lambda)\mathrm{d}\lambda = 1$. Since the bandwidth of the spectrograph or detector used in the MME system is less than several nanometers, the optical properties of the compensator can be represented by the first-order Taylor expansion:

$$\begin{aligned} \delta(\lambda + \Delta\lambda) &= \delta_\lambda + \dot{\delta}_\lambda\Delta\lambda \\ \theta(\lambda + \Delta\lambda) &= \theta_\lambda + \dot{\theta}_\lambda\Delta\lambda \\ \rho(\lambda + \Delta\lambda) &= \rho_\lambda + \dot{\rho}_\lambda\Delta\lambda \end{aligned} \tag{9}$$

where $\dot{\delta}_\lambda$, $\dot{\theta}_\lambda$, and $\dot{\rho}_\lambda$ represent the first-order derivative of the compensator's retardance, azimuthal angle, and rotary angle with respect to the wavelength λ respectively. Consequently, the integral in equation (8) can be simplified as:

$$\overline{\mathbf{M}}(\lambda) = \mathbf{R}(-\rho_\lambda)\mathbf{R}(-\theta_\lambda)\mathbf{M}_{\mathrm{act}}(\delta_\lambda)\mathbf{R}(\theta_\lambda). \tag{10}$$

Here, we define $\mathbf{M}_{\mathrm{act}}(\delta_\lambda)$ as the actual Mueller matrix of the compensator at wavelength λ by taking into account the bandwidth effect, with a general formula of

$$\mathbf{M}_{\mathrm{act}}(\delta_\lambda) = \begin{bmatrix} 1 & 0 & 0 & 0 \\ 0 & d_1 & 0 & 0 \\ 0 & 0 & d_2\cos\delta_\lambda & d_3\sin\delta_\lambda \\ 0 & 0 & -d_4\sin\delta_\lambda & d_5\cos\delta_\lambda \end{bmatrix}, \tag{11}$$

where d_i $(i = 1,\ldots5)$ are defined as the depolarization parameters,

$$\begin{aligned} d_1 &= \int w(\lambda + \Delta\lambda)\cos[2(\dot{\rho}_\lambda - \dot{\theta}_\lambda)\Delta\lambda] \\ &\quad\times \cos(2\dot{\theta}_\lambda\Delta\lambda)\mathrm{d}\Delta\lambda \\ d_2 &= \int w(\lambda + \Delta\lambda)\cos[2(\dot{\rho}_\lambda - \dot{\theta}_\lambda)\Delta\lambda] \\ &\quad\times \cos(2\dot{\theta}_\lambda\Delta\lambda)\cos(\dot{\delta}_\lambda\Delta\lambda)\mathrm{d}\Delta\lambda \\ d_3 &= \int w(\lambda + \Delta\lambda)\cos[2(\dot{\rho}_\lambda - \dot{\theta}_\lambda)\Delta\lambda] \\ &\quad\times \cos(\dot{\delta}_\lambda\Delta\lambda)\mathrm{d}\Delta\lambda \\ d_4 &= \int w(\lambda + \Delta\lambda)\cos(2\dot{\theta}_\lambda\Delta\lambda)\cos(\dot{\delta}_\lambda\Delta\lambda)\mathrm{d}\Delta\lambda \\ d_5 &= \int w(\lambda + \Delta\lambda)\cos(\dot{\delta}_\lambda\Delta\lambda)\mathrm{d}\Delta\lambda. \end{aligned} \quad (12)$$

The significance of equation (11) is that the introduced depolarization parameters d_i of the Mueller matrix can be directly related to its depolarization index. Actually, by inserting equation (11) into equation (3), we can immediately obtain the relationship as:

$$DI = \left[\frac{d_1^2 + (d_2^2 + d_5^2)\cos^2\delta_\lambda + (d_3^2 + d_4^2)\sin^2\delta_\lambda}{3}\right]^{1/2}. \quad (13)$$

Apparently, the value of the depolarization parameters d_i is always less than 1 unless the derivatives of the compensator's retardance, azimuthal angle, and rotary angle are all 0, which means that these optical properties should be wavelength-independent.

In practice, the calculation of equation (12) requires discretization in the range of wavelength at all specified discrete points followed by weighted averaging. The function $w(\lambda)$ can be selected as a Gaussian function [21] with a bandwidth such as 3.5 nm in our case. The values of the retardance, the azimuthal angle, and the rotary angle of the compensator can be obtained from a calibration procedure based on the regression calibration method [22], by performing a measurement on a standard film, e.g. a SiO_2 thermal oxide film on a Si substrate. Figure 4 shows the values of these three optical properties of the 1st rotating compensator in our MME system. As expected, the optical properties are indeed wavelength-dependent due to the chromatic dispersion of the materials. Thus the depolarization parameter d_i, and consequently the depolarization index of the compensator is less than 1. It is therefore demonstrated that the depolarization effects are essentially artifacts and are mainly induced by the wavelength dependence of the compensator's optical properties and the finite bandwidth of the MME system.

Figure 5 shows the depolarization parameters of the 1st rotating compensator calculated by the optical properties shown in figure 4 with an instrument bandwidth of 3.5 nm. It can be observed that the depolarization parameters d_1, d_2 and d_3 have similar values, and so do the depolarization parameters d_4 and d_5. This is mainly because of the small bandwidth in our MME system and is expected in the

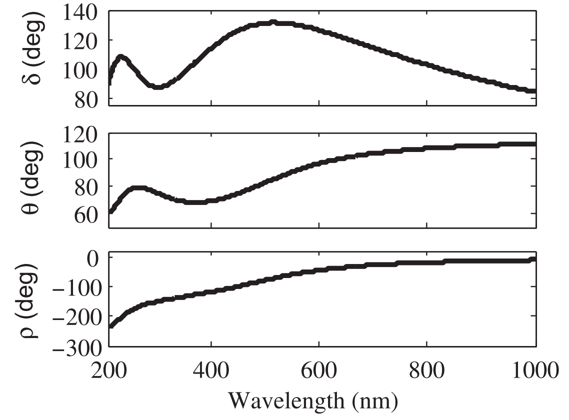

Figure 4. Retardance, azimuthal angle, and rotary angle of the 1st rotating compensator.

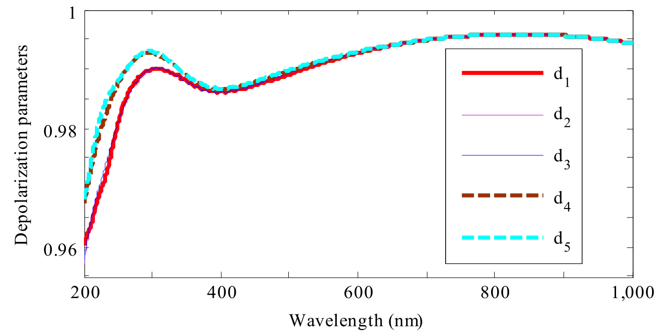

Figure 5. Depolarization parameters of the 1st rotating compensator.

definitions shown in equation (12). To eliminate the depolarization artifacts in the MME system, the actual Mueller matrix expressed in equation (11) is used for the compensator instead of the ideal formulation shown in equation (6). To simplify the calculation, equation (11) can be further simplified as

$$\mathbf{M}_{\mathrm{act}}(\delta_\lambda) = \begin{bmatrix} 1 & 0 & 0 & 0 \\ 0 & a & 0 & 0 \\ 0 & 0 & a\cos\delta_\lambda & a\sin\delta_\lambda \\ 0 & 0 & -b\sin\delta_\lambda & b\cos\delta_\lambda \end{bmatrix} \quad (14)$$

where the parameter a is the average value of the depolarization parameters d_1, d_2 and d_3, and the parameter b is the average value of the depolarization parameters d_4 and d_5.

4. Correction of depolarization artifacts in DRC-MME

By incorporating the general formula of the actual compensator into the system model shown in equation (1), the output Stokes vector $\mathbf{S}_{\mathrm{out}}$ of the light beam exiting the analyzer can

Table 1. The relationship between the sample Mueller matrix elements m_{jk} and the corresponding pseudo Mueller matrix elements m'_{jk}.

$m'_{11} = 1$	$m'_{12} = m_{12}/(a_1)$	$m'_{13} = m_{13}/(a_1)$	$m'_{14} = m_{14}/(b_1)$
$m'_{21} = m_{21}/(a_2)$	$m'_{22} = m_{22}/(a_1 a_2)$	$m'_{23} = m_{23}/(a_1 a_2)$	$m'_{24} = m_{24}/(a_2 b_1)$[a]
$m'_{31} = m_{41}/(a_2)$	$m'_{32} = m_{32}/(a_1 a_2)$	$m'_{33} = m_{33}/(a_1 a_2)$	$m'_{34} = m_{34}/(a_2 b_1)$
$m'_{41} = m_{41}/(a_2)$	$m'_{42} = m_{42}/(a_1 a_2)$	$m'_{43} = m_{43}/(a_1 a_2)$	$m'_{44} = m_{44}/(a_2 b_1)$

[a] a_p and b_p ($p = 1, 2$) represent the depolarization parameters of the 1st and 2nd rotating compensators respectively.

be expressed as:

$$\mathbf{S}_{\text{out}} = [\mathbf{M}_A \mathbf{R}(A')][\mathbf{R}(-C_2')\mathbf{M}_{C_2}(\delta_2)\mathbf{R}(C_2')] \times \mathbf{M}_S \times [\mathbf{R}(-C_1')\mathbf{M}_{C_1}(\delta_1)\mathbf{R}(C_1')] \times [\mathbf{R}(-P')\mathbf{M}_P\mathbf{R}(P')]\mathbf{S}_{\text{in}}. \tag{15}$$

Due to the influence of the compensator's rotary angle, the azimuthal angle corresponding to the analyzer, the compensators, and the polarizer will vary as $A' = A + \rho_2$, $C_2' = C_2$, $C_1' = C_1 - \rho_1$, and $P' = P - \rho_1$, where ρ_1 and ρ_2 represent the rotary angle of the 1st and 2nd rotating-compensator respectively. By multiplying the matrices in equation (15), we can obtain the following expression for the irradiance at the detector, which is proportional to the first element of $\mathbf{S}_{\text{out}}$:

$$I = I_0\{K_1 + [c_2 \cos 2A' + s_2 \cos(4C_2' - 2A')]K_2 + [c_2 \sin 2A' + s_2 \sin(4C_2' - 2A')]K_3 - \sin\delta_2 \sin 2(C_2' - A')K_4\}, \tag{16a}$$

where

$$K_j = m_{j1} + [c_1 \cos 2P' + s_1 \cos(4C_1' - 2P')]m_{j2} + [c_1 \sin 2P' + s_1 \sin(4C_1' - 2P')]m_{j3} + \sin\delta_1 \sin 2(C_1' - P')m_{j4}. \tag{16b}$$

Here, $c_i = \cos^2(\delta_i/2)$ and $s_i = \sin^2(\delta_i/2)$ $(i = 1, 2)$. In equation (16), m_{jk} $(j = 1,\ldots 4;\ k = 1,\ldots 4)$ are the elements of the pseudo sample Mueller matrix and have a relationship with the corresponding sample Mueller matrix elements m'_{jk} as shown in table 1. By assuming all the conditions to be ideal, [13] gave the exactly same expressions as in equation (16). Consequently, we can calculate the pseudo Mueller matrix elements using the equations deduced in [13], and then achieve the actual Mueller matrix of the sample as shown in table 1.

Figure 6 shows the spectroscopic Mueller matrix measurement of the air (normalized to the m_{11} element) calculated by the proposed correction method. It is noted that the deviation from the theoretical identity matrix is extremely small, and the error is less than 0.2% over most of the spectrum, and the standard deviation is no more than 0.1%. Comparing the Mueller matrix spectra shown in figures 2 and 6, it is obvious that much smaller deviations from the identity matrix are achieved by performing the proposed correction method. Figure 7 depicts the comparison of the depolarization index spectrum with and without the proposed correction method. The corrected depolarization indices are very close to

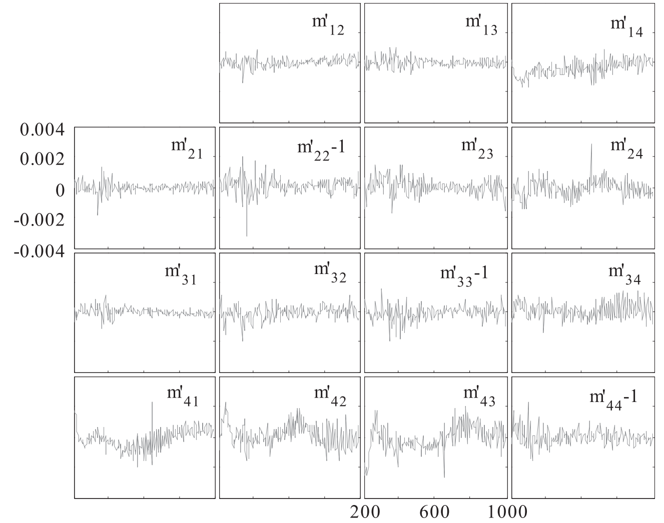

Figure 6. Mueller matrix spectra calculated with the proposed correction method. The Mueller matrix elements are normalized to m_{11}, which is not shown. The horizontal axes, varying from 200 to 1000 nm, denote the wavelengths, and the vertical axes denote the values of the associated Mueller matrix elements. The diagonal elements m_{22}, m_{33} and m_{44} are minus 1 for the convenience of unified coordinate axis.

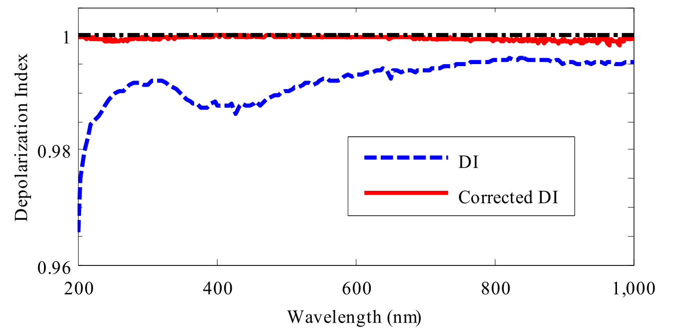

Figure 7. Depolarization index spectra of the ellipsometer-measured Mueller matrix spectra with and without the proposed correction method.

1 in the entire spectral range, which means that the corrected Mueller matrix spectra are nearly non-depolarizing matrices.

For further demonstration, we measure an MgF_2 rochon polarizer with MME using the straight-through mode and a SiO_2 film on silicon substrate using the reflective measurement mode, respectively. The azimuthal angle of the polarizer, which denotes the angle between the transmission axis of polarizer and the x axis, is set to be 5.4° in the first experiment. The incident angle is set to be 65° in the second experiment and the nominal thickness of the SiO_2 film is

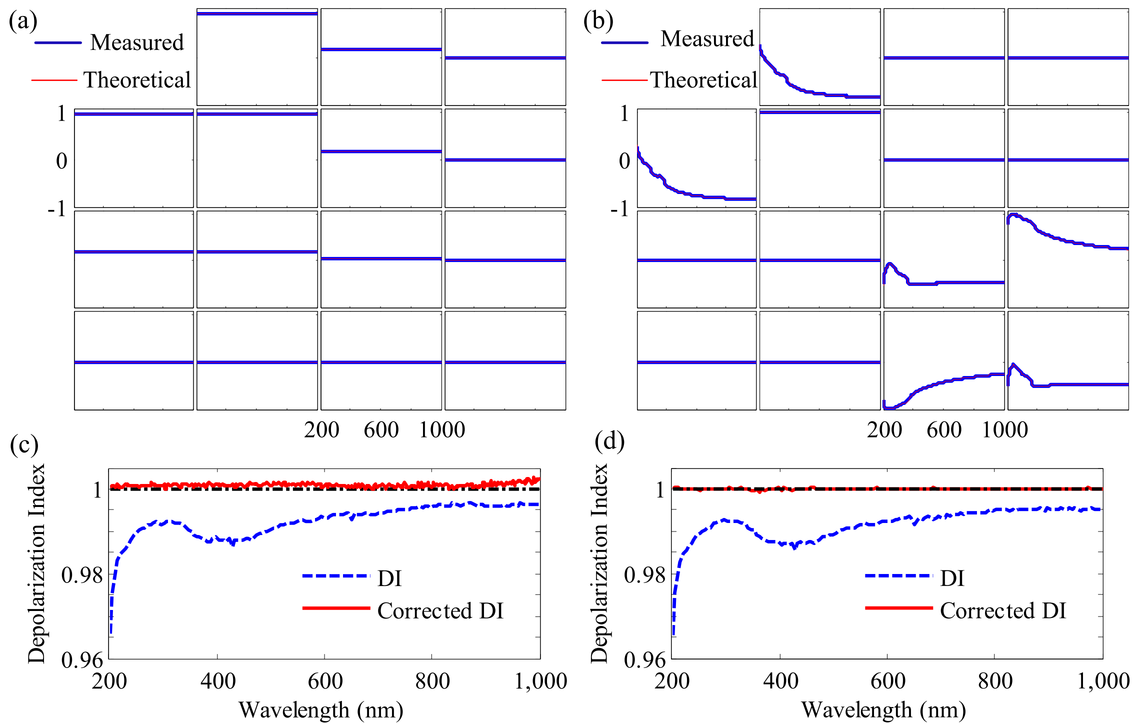

Figure 8. Corrected Mueller matrix with the proposed method and the theoretical data of (a) the MgF_2 rochon polarizer and (b) the SiO_2 film. And depolarization index spectra of the ellipsometer-measured Mueller matrix spectra obtained on (c) the MgF_2 rochon polarizer and (d) the SiO_2 film with and without the proposed correction method.

24.88 nm. Figures 8(a) and (b) show the corrected Mueller matrix with the proposed method, and the theoretical fitting data of the polarizer and the SiO_2 film. As can be seen, good agreements have been achieved in both experiments. The corresponding depolarization indices with and without performing the correction are shown in figures 8(c) and (d) for comparison. It can be observed that the corrected depolarization indices approximate to 1 within the broad spectral range, which indicates the corrected Mueller matrices are nearly non-depolarizing matrices. It thus further demonstrates that the proposed correction method eliminates the depolarization artifacts in the measurement. Consequently, significant improvement in accuracy has been achieved.

5. Conclusion

In summary, obvious depolarization effects have been observed from the measurement of the air using an in-house developed DRC-MME system. We have demonstrated that these depolarization effects are essentially artifacts and mainly induced by the wavelength-dependent properties of the compensator and the finite bandwidth of the system. By incorporating these effects into the optical model, we have proposed a correction method to eliminate the depolarization artifacts. The experiment performed on the MME system has demonstrated the validity of the proposed method, and consequently, improved accuracy has been achieved in the Mueller matrix measurement.

Acknowledgments

This work was funded by the National Natural Science Foundation of China (51475191, 51405172, 51575214, and 51525502), the Provincial Natural Science Foundation of Hubei (2015CFB278 and 2015CFA005), and the Program for Changjiang Scholars and Innovative Research Team in University of China (IRT13017).

References

[1] Chen C, An I and Collins R W 2003 Multichannel mueller matrix ellipsometry for simultaneous real-time measurement of bulk isotropic and surface anisotropic complex dielectric functions of semiconductors *Phys. Rev. Lett.* **90** 217402
[2] Stchakovsky M, Caillaud C, Foldyna M, Ossikovski R and Garcia-Caurel E 2008 Polarimetric characterization of optically anisotropic flexible substrates *Thin Solid Films* **516** 1414
[3] Berrier A, Gompf B, Fu L W, Weiss T and Schweizer H 2014 Optical anisotropies of single-meander plasmonic metasurfaces analyzed by Mueller matrix spectroscopy *Phys. Rev.* B **89** 195434
[4] Novikova T, De Martino A, Bulkin P, Nguyen Q, Drevillon B, Popov V and Chumakov A 2007 Metrology of replicated diffractive optics with Mueller polarimetry in conical diffraction *Opt. Express* **15** 2033
[5] Chen X, Liu S, Zhang C, Jiang H, Ma Z, Sun T and Xu Z 2014 Accurate characterization of nanoimprinted resist patterns using Mueller matrix ellipsometry *Opt. Express* **22** 15165

[6] Chen X, Zhang C, Liu S, Jiang H, Ma Z and Xu Z 2014 Mueller matrix ellipsometric detection of profile asymmetry in nanoimprinted grating structures *J. Appl. Phys.* **116** 194305
[7] Foldyna M, De Martino A, Ossikovski R, Garcia-Caurel E and Licitra C 2009 Characterization of grating structures by Mueller polarimetry in presence of strong depolarization due to finite spot size *Opt. Commun.* **282** 735
[8] Chen X, Zhang C and Liu S 2013 Depolarization effects from nanoimprinted grating structures as measured by Mueller matrix polarimetry *Appl. Phys. Lett.* **103** 151605
[9] Hauge P S 1978 Mueller matrix ellipsometry with imperfect compensators *J. Opt. Soc. Am.* **68** 1519
[10] Goldstein D H and Chipman R A 1990 Error analysis of a Mueller matrix polarimeter *J. Opt. Soc. Am.* A **7** 693
[11] Lee J, Rovira P I, An I and Collins R W 2001 Alignment and calibration of the MgF_2 biplate compensator for applications in rotating-compensator multichannel ellipsometry *J. Opt. Soc. Am.* A **18** 1980
[12] Broch L, Naciri A E and Johann L 2008 Systematic errors for a Mueller matrix dual rotating compensator ellipsometer *Opt. Express* **16** 8814
[13] Collins R W and Koh J 1999 Dual rotating-compensator multichannel ellipsometer: instrument design for real-time Mueller matrix spectroscopy of surfaces and films *J. Opt. Soc. Am.* A **16** 1997
[14] Fujiwara H 2007 *Spectroscopic Ellipsometry: Principles and Applications* (New York: Wiley)
[15] Liu S, Chen X and Zhang C 2015 Development of a broadband Mueller matrix ellipsometer as a powerful tool for nanostructure metrology *Thin Solid Films* **584** 176
[16] Smith M H 2002 Optimization of a dual-rotating-retarder Mueller matrix polarimeter *Appl. Opt.* **41** 2488
[17] Gil J J and Bernabeu E 1986 Depolarization and polarization indexes of an optical system *Opt. Acta* **33** 185
[18] Azzam R M A and Bashara N M 1977 *Ellipsometry and Polarized Light* (Amsterdam: North-Holland)
[19] Hurwitz H Jr and Jones R C 1941 A new calculus for the treatment of optical systems: II. Proof of three general equivalence theorems *J. Opt. Soc. Am.* **31** 493
[20] Gu H, Liu S, Chen X and Zhang C 2015 Calibration of misalignment errors in composite waveplates using Mueller matrix ellipsometry *Appl. Opt.* **54** 684
[21] Germer T A and Patrick H J 2010 Effect of bandwidth and numerical aperture in optical scatterometry *Proc. SPIE* **7638** 76381F
[22] Johs B D 1993 Regression calibration method for rotating element ellipsometers *Thin Solid Films* **234** 395